WHOI-79-90 C.2

Woods Hole
Oceanographic
Institution

NEAR-SURFACE OCEAN CURRENT SENSORS: PROBLEMS AND PERFORMANCE

by

James R. McCullough

December 1979

TECHNICAL REPORT

Prepared for the Working Conference on CURRENT MEASUREMENTS sponsored by the NOAA Office of Ocean Engineering with the Delaware Sea Grant College Program.

WOODS HOLE, MASSACHUSETTS 02543

WHOI-79-90

NEAR-SURFACE OCEAN CURRENT SENSORS: PROBLEMS AND PERFORMANCE

James R. McCullough
Woods Hole Oceanographic Institution
Woods Hole, Massachusetts 02543

December 1979

TECHNICAL REPORT

Prepared for the Working Conference on CURRENT MEASUREMENTS sponsored by the NOAA Office of Ocean Engineering with the Delaware Sea Grant College Program.

Reproduction in whole or in part is permitted for any purpose of the United States Government. This report should be cited as: Woods Hole Oceanographic Institution Technical Report, WHOI-79-90.

Approved for Distribution

Valentine Worthington, Chairman
Dept. of Physical Oceanography

Table of Contents

Abstract

When current meters are used to measure mean horizontal currents in surface gravity waves, immunity to the vertical component of flow is important, even though the net vertical flow averages to zero and is normal to the desired horizontal components. A technique is presented for estimating the magnitude of the errors introduced by imperfect rejection of the off-axis flows (cross-talk) from laboratory measurements of the current meter "vertical-cosine-response." The predicted dynamic response is shown to compare favorably with laboratory measurements. The measured steady state vertical-cosine-response functions for several practical current sensors are summarized and used to estimate the magnitude of wave-induced errors in horizontal mean current measurements. A new dye technique for evaluating near-surface current meter performance in waves is shown.

1. Introduction

Ocean currents can now be measured routinely in all but the strongest flows and in the surface wave zone. In the wave zone, the orbital velocities require greater sensor linearity than has, until very recently, been available. McCullough (1978), Davis and Weller (1978), Smith (1974), and others describe acoustic and propeller sensors which show considerable promise for wave zone measurements.

It may seem strange that flow measurements in waves are difficult to make, when both time and distance can be measured with extraordinary accuracy. The difficulty arises naturally from the broadband nature of the wave zone flow. There is no single speed present, but rather a mixture of speeds and length scales characterized by their broad frequency, amplitude, and wavenumber spectra. Implicit then in the concept of fluid "velocity" is knowledge of the averaging processes (time and space) used in making the measurement. The nature of errors introduced by improper averaging in the presence of surface gravity waves and/or wave-driven mooring motion is the subject of this paper.

2. The Signal

Figure 1 shows the nature of the near-surface flow signal as inferred (a) photographically, (b-c) from pressure measurements, and (d) as measured directly with current meters. Wave flow in a "sea" is seen to be very complex, quite unlike the periodic linear motions traditionally used to model it. Note the similarity of wave shape over a wide range of wave scales (from 0.5 m waves in (c), to 10 m waves in (b)). The v and w (horizontal and vertical) speeds shown in (d) give some feeling for the signal at 2 m depth as seen from a rigid platform. In other records of this type, Shonting (1967) shows that even the approximate 90° phase relation between v and w is not always maintained from wave to wave.

Figure 2 shows a typical frequency distribution of flow energy near the ocean surface. The term ocean "currents" is conventionally used to describe motions such as those of the tidal, inertial, and lower frequency processes shown at the left. To measure these currents in the presence of the large wave energies shown at the right, some form of frequency separation (usually vector averaging) is employed to reduce the current meter bandwidth. The separation is made practical by the low energy "gap" at frequencies of roughly 1 to 10 cycles

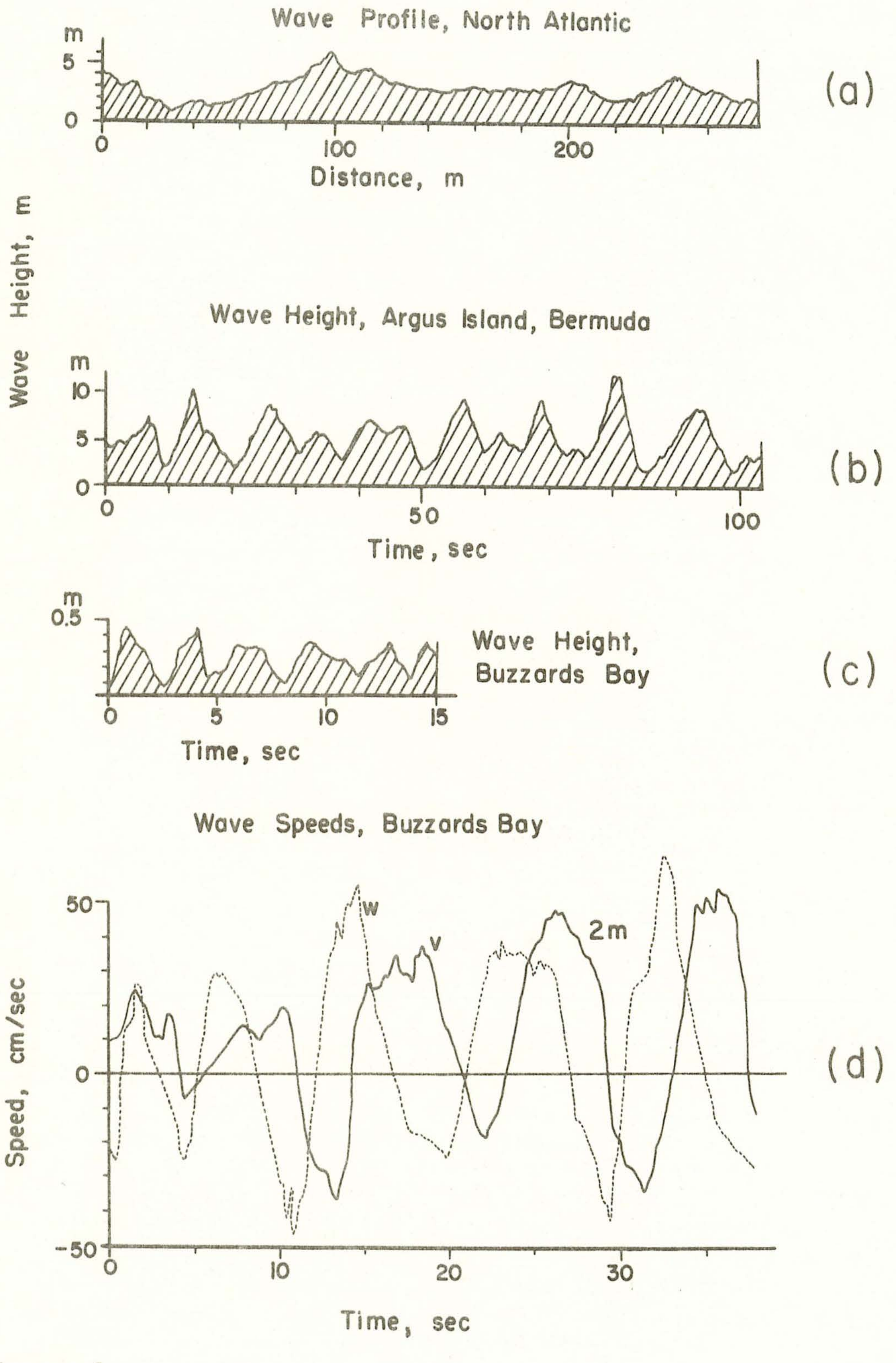

Figure 1

Measured wave signals from: (a) stereoscopic photographs; (b) and (c) tower mounted pressure gauges; and (d) direct propeller speed observations from a fixed tower at 2 m depth in small waves. "Sea" waves are seen to be highly irregular in space, time, and speed. [Frames (a-c) after Neumann and Pierson, 1966; frame (d) after Shonting, 1967.]

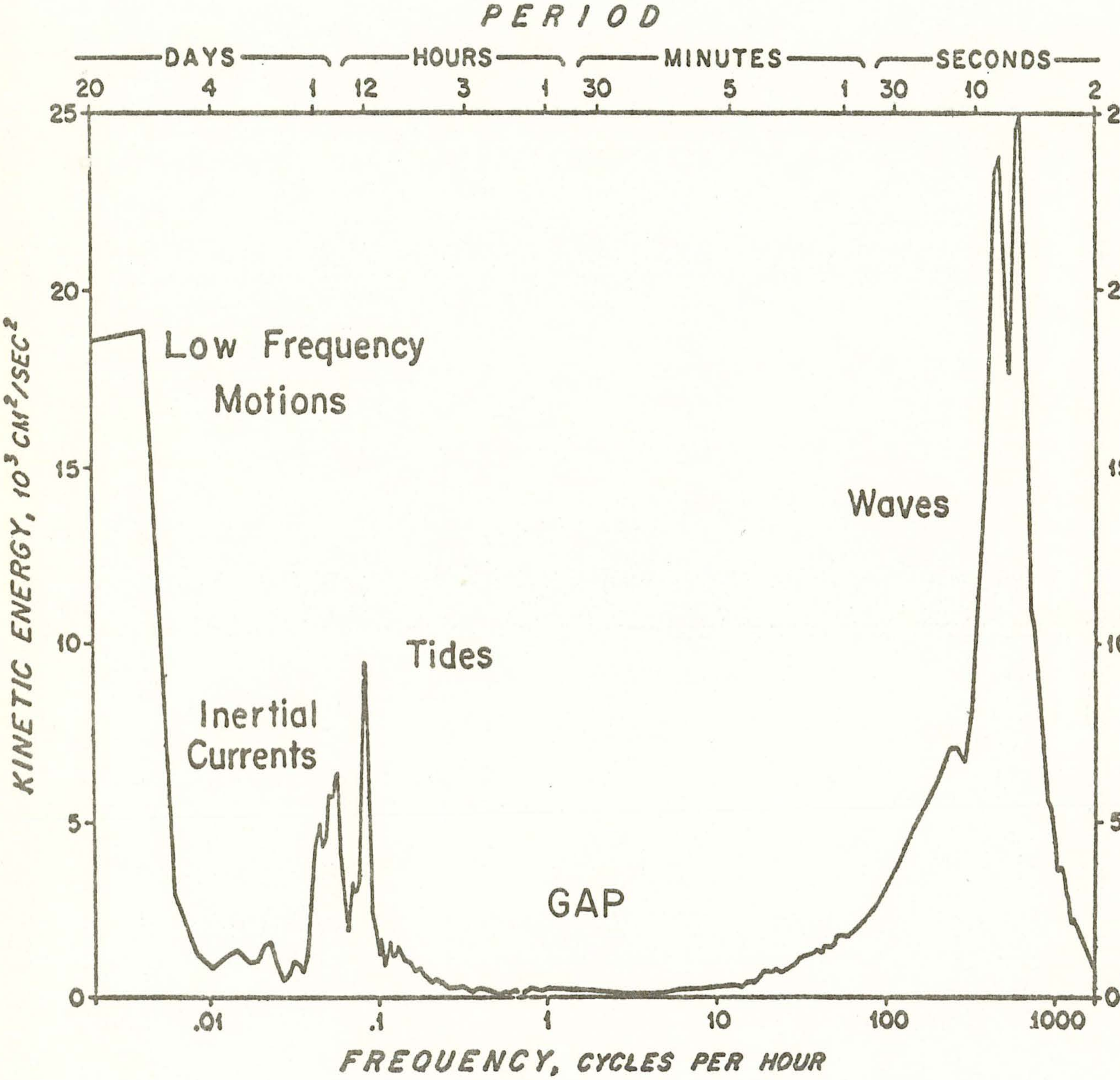

Figure 2

Typical distribution of energy near the ocean surface as a function of frequency (and period). The data are scaled so that equal areas under the curve represent equal energies, i.e., a "variance preserving" plot. To correctly measure the lower frequency tides, etc. (left), it is necessary to follow the wave motions (right) even though they average to zero (after Webster, 1967).

per hour. To limit the scope of the discussion here, current meters are assumed to register only the mean horizontal component of current below wave frequencies, i.e., the part of the signal to the left of the wave energy in Figure 2.

3. Vector Averaging

Figure 3 further illustrates the importance of low-pass velocity component filtering (vector averaging) in the wave zone. Note that the rotor (scalar) speeds of the vector averaging current meter (VACM) are large, while the magnitude of the vector-averaged velocity varies from nearly that of the rotor on May 1, to two (or more) orders of magnitude less on May 10. For this reason, current meters which use separate speed and direction averaging schemes (Aanderaa, Alexaev, Hydro Products, etc.) are generally not considered suitable for measuring mean velocity in the wave zone.

4. Sensor Response

Figure 4 illustrates the improvement in sensor response that can be expected with acoustic-travel-time-difference sensors as compared with rotors. Laboratory measurements of rotors have for some time shed doubt on the validity of all rotor-vane measurements in waves. As will be suggested in the discussion of Figure 13, such reservations may be overly conservative since the laboratory tests may inadequately model broadband wave flows seen from moving moorings.

5. A Kinematic Model of Vertical-Cosine-Response

The importance of current meter vertical-cosine-response is illustrated in Figures 5 through 9. The term vertical-cosine-response is used to describe a current meter's ability to reject vertical components of flow while making horizontal flow measurements, i.e., to measure only the component $V \cos\theta$, of flow V at an angle θ to the horizontal plane. Figure 5 introduces the model concept. The model is used to estimate mean horizontal dynamic response from steady flow measurements of vertical-cosine-response. The analysis treats only the kinematics of the problem and does not include important dynamic considerations such as sensor wake variations and response in turbulence.

At the top of Figure 5, the modeled circular wave orbital velocities ($a\omega$) are added to mean speeds (V_0). The speeds S are then numerically integrated to find the average velocity

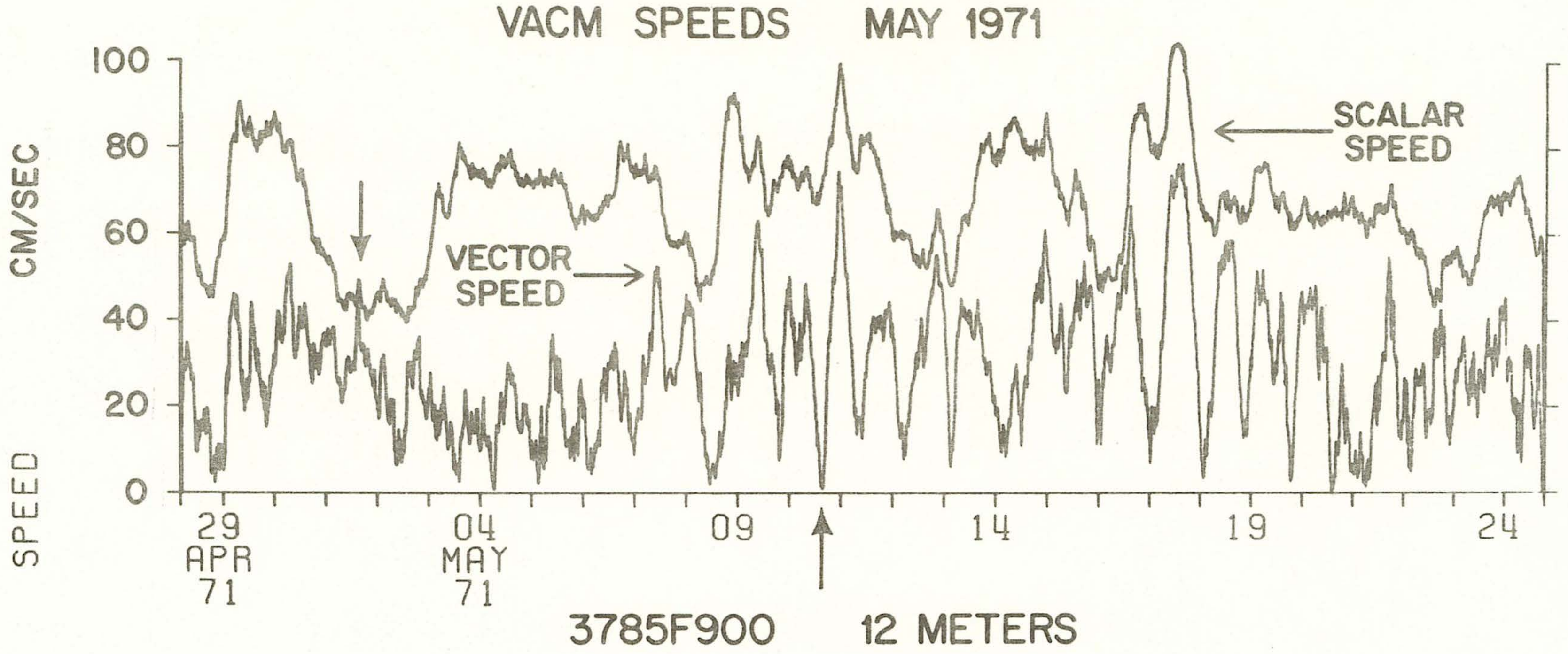

Figure 3

Vector averaging current meter (VACM), 15-minute averaged rotor speed, and vector magnitude at 12 m depth below a surface-following toroid float in 2665 m of water at WHOI Site D, May 1971. Note that the rotor speed from one 15-minute sample to the next is nearly constant (the rotor curve is relatively smooth from hour to hour). Also note that the vector magnitude found by including several thousand compass and vane samples each 15 minutes is often much smaller than that of the rotor value. On 10 May, for example, the indicated vector average nearly goes to zero even though the rotor is turning at nearly 70 cm/sec (after McCullough, 1975).

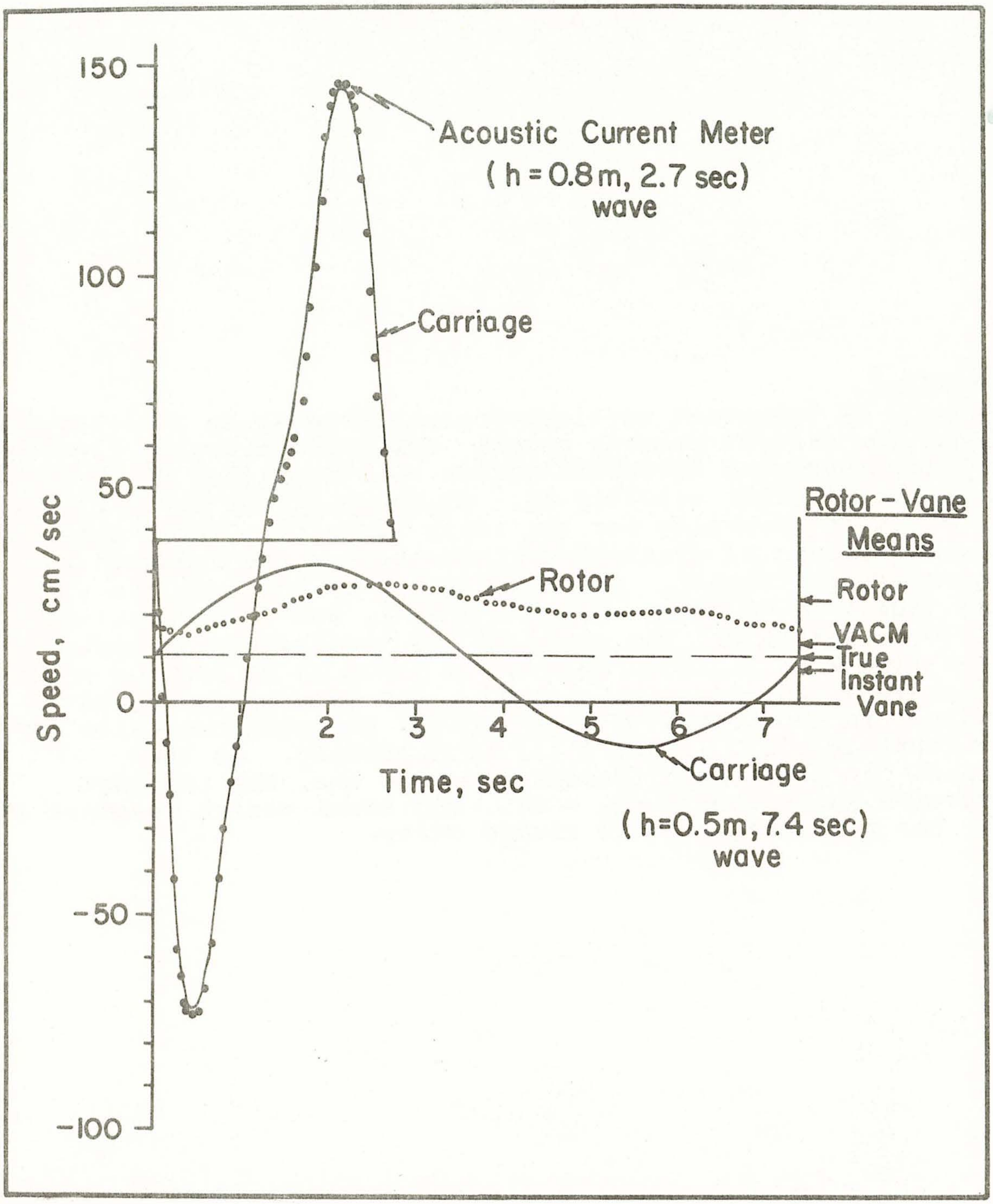

Figure 4

Dynamic tow tank data from an acoustic-travel-time-difference current meter and a VACM. The acoustic meter (upper dotted curve) follows the carriage coplanar sloshing motion almost exactly, while the rotor (lower dotted curve) runs nearly twice as fast as the true mean value shown at the right. Also at the right, if the vane response were instantaneous (no lag), the computed mean value would be too small. The mean found by the lagged vane of the VACM, however, is somewhat too large. If the vane had not reversed, the mean would be that of the rotor, which is too large by about a factor of 2. (After McCullough, 1974, and more recent unpublished data.)

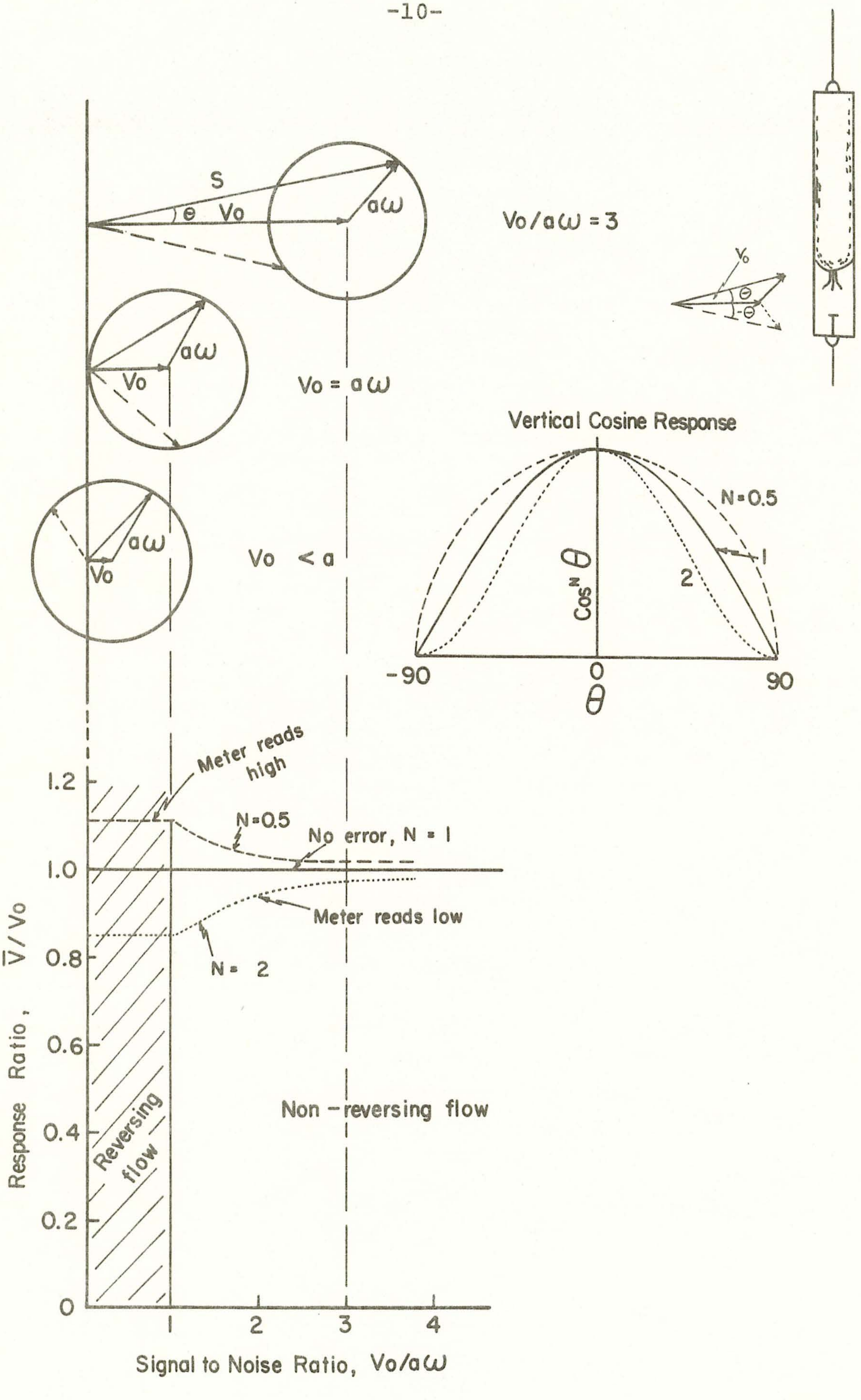
S
θ
Vo
aω
Vo/aω = 3
Vo
θ
-θ
aω
Vo
Vo = aω
Vertical Cosine Response
N=0.5
1
2
$\cos^N \theta$
-90
0
90
θ
aω
Vo
Vo < a
Meter reads high
N=0.5
No error, N = 1
Meter reads low
N = 2
1.2
1.0
0.8
0.6
0.4
0.2
0
Response Ratio, $\overline{V}$/Vo
Reversing flow
Non-reversing flow
1
2
3
4
Signal to Noise Ratio, Vo/aω

($\overline{V}$) of meters with imperfect vertical-cosine-response. Since the direction errors introduced by inaccurate vertical-cosine-response are generally small (∿5° or less in the example shown), only the speed component of $\overline{V}$ is shown.

The model results are parameterized by the response ratio $\overline{V}/V_O$ (the ratio of measured to true mean speed), and the flow "signal-to-noise ratio", $V_o/a\omega$ (the ratio of the steady to the oscillatory flow speeds[1]). The three circular diagrams at the top of Figure 5 give example flows to help visualize the ratio $V_O/a\omega$. Two assumed departures from ideal vertical-cosine-response are shown at the top right. The bottom graph gives the modeled mean response of the meters in single-frequency, circular-orbital waves which are coplanar with the mean velocity V_O. For signal-to-noise ratios less than one ($V_o/a\omega < 1$), reversing flows are indicated.

Critical values of the response ratio and signal-to-noise ratio exist at values of <u>ONE</u>. The line $\overline{V}/V_O = 1$ represents the locus of all correct readings. As will be shown next, the vertical line $V_O/a\omega = 1$ separates regions of high and low dependence on wave orbit characteristics.

Figure 6 extends the coplanar circular-motion of the previous figure to more general cases including orbital motion at an angle to the mean flow (the usual case) and elliptical motion (such as seen from a surface following mooring).

A collection of various calculated responses is shown in Figure 7a. For signal-to-noise ratios less than "one" (to the left of the vertical dash-line), a wide range of error conditions exists depending on the wave and mean current geometries. For values greater than "one," such considerations are of little importance.

Figure 7b shows that typical near-surface ocean conditions place high demands on rigidly mounted current meters. The actual moored situation modeled later in Figure 11 is more complex, but at shallow depths is less demanding.

Figure 8 shows <u>measured</u> vertical-cosine-response functions of four practical ocean current sensors tested at the David Taylor Naval Ship Research and Development Center (DT-NSRDC).

---

[1] The flow "signal-to-noise ratio" as used here is <u>not</u> the same as the usual instrument signal-to-noise ratio.

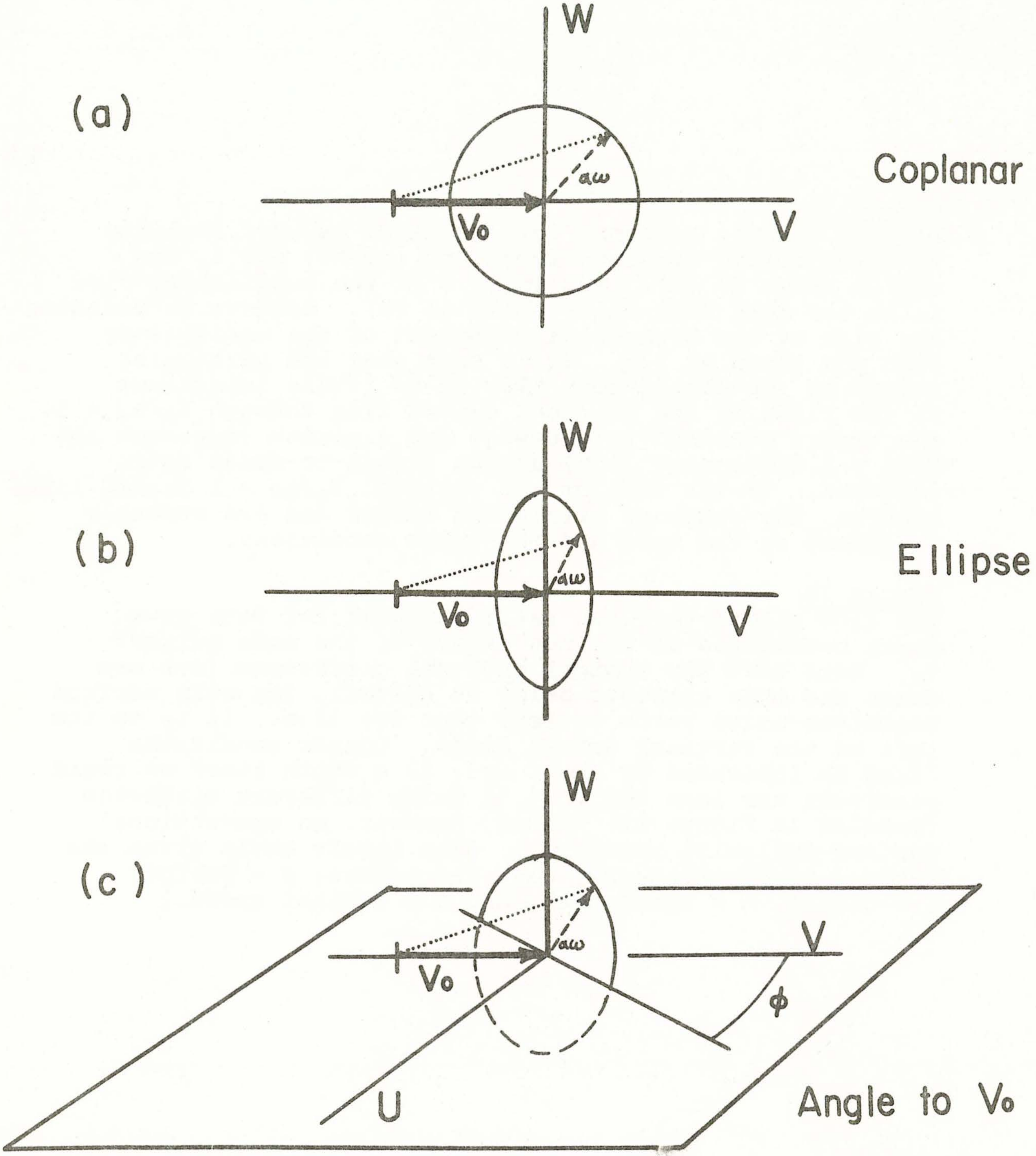

Figure 6

Three cases of orbital and steady motion are considered in Figures 7-9: (a) coplanar V_o and circular $a\omega$; (b) elliptical motion as might be seen at moderate or mid-depths on a surface-following mooring; and (c) orbital motion (circular or elliptical) at an angle ϕ (in the horizontal plane) to V_o.

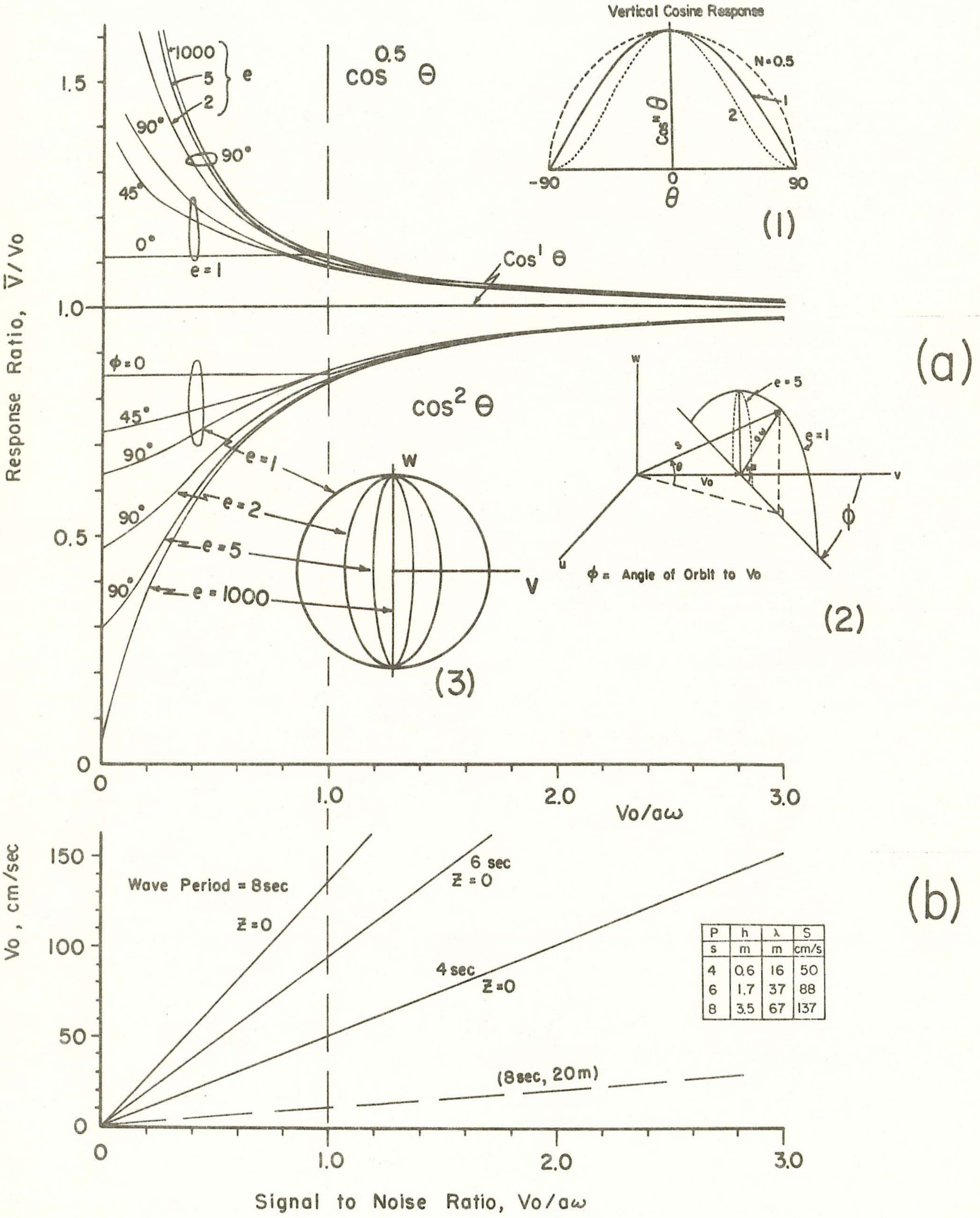

P	h	λ	S
s	m	m	cm/s
4	0.6	16	50
6	1.7	37	88
8	3.5	67	137

The functions have been used as input to the numeric model to predict error components due to improper vertical-cosine-response. From the 12 curves labeled c, n, and ℓ (for coplanar, normal, and linear-normal oscillations respectively), it is clear that the predicted errors are complex functions of the flow signal-to-noise ratio and can be large at low signal-to-noise ratios. This complexity may help account for some of the puzzling response variability frequently noted in *in situ* wave zone intercomparisons. Halpern (1977 and 1978) reviews such *in situ* intercomparisons. Note that low values of $V_o/a\omega$ do not necessarily imply small (insignificant) mean speeds V_o.

Figure 9 shows the general agreement between predicted and measured dynamic response for a prototype acoustic-travel-time-difference meter. The agreement with the model suggests the importance of vertical-cosine-response in such meters.

6. Some Measured Dynamic Response Functions of Current Sensors

Figure 10 compares the *measured* dynamic response of four popular types of current sensors, plotted in the same coordinates used in the previous figures. At low signal-to-noise ratios, the particular electromagnetic and rotor-vane systems shown (top) overestimate speeds, while the propellers and acoustic sensors (bottom) tend to underestimate the mean.

7. Errors Due to Mooring Motion

Figure 11 (top left) shows the Stokes-drift and error due to surface following *vertical*-mooring-motion as a function of depth, for the arbitrary long swell condition indicated. Ideal current meters (ones with no errors), no lateral mooring motion, and monochromatic waves are assumed in this case. The predicted mooring-induced errors are seen to be relatively small. In other situations, particularly very near the surface in high seas or at mid-depths on surface-following moorings, the motion-induced errors may be dominant. (For further discussion of the Stokes-drift and mooring motion effects see Kenyon, 1969; Pollard, 1973; Ianniello and Garvine, 1975; Carson and Collar, 1977, etc.)

The exponential decay of the wave-orbital horizontal and vertical speed components, u' and w' (Figure 11, upper right), is also shown as a function of depth. In typical deep-sea wire-moorings, the vertical-mooring-motion (w) is essentially

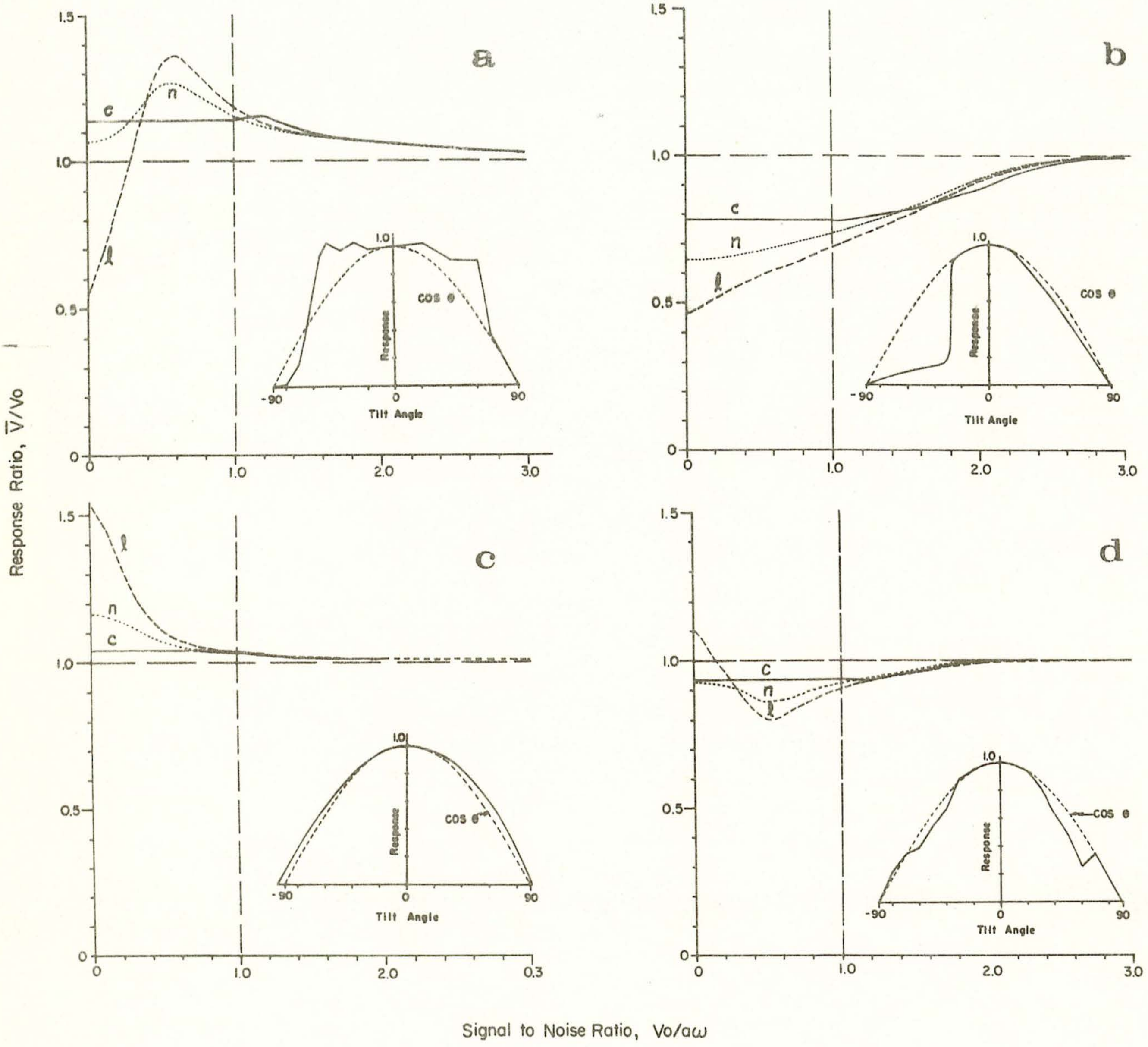

Figure 8

Modeled dynamic response calculated for four measured steady-state vertical-cosine response functions. a) A one-inch diameter cylindrical electromagnetic probe between flat circular end plates. b) A disc-shaped electromagnetic sensor. c) The same probe as in (a) less the end plates. d) An acoustic-travel-time-difference probe of the mirror type. The measured static response functions are shown in the insert of each frame. The curves labeled c, n, and ℓ represent coplanar ($\phi = 0°$) and normal ($\phi = 90°$) circular orbits, and linear (large e) sinusoidal motion respectively. As before, the vertical dashed lines separate regions of high and low sensitivity to the orientation and shape of the oscillatory flow. (Panel inserts a, b, and c after McCullough, 1974; d after Appell, 1977a.)

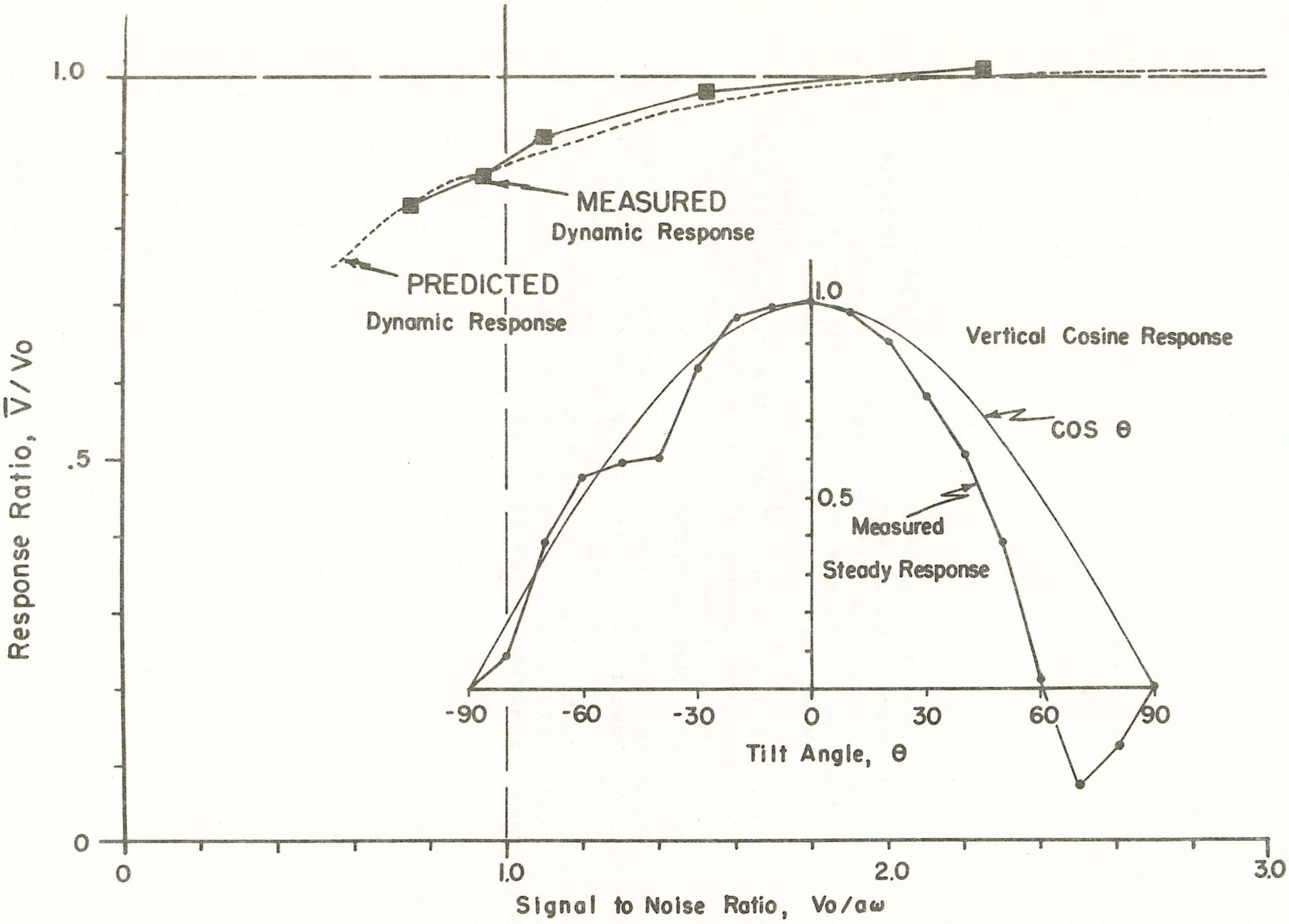

Figure 9

Model verification is demonstrated by general agreement of predicted and measured dynamic response of an experimental mirror-type acoustic-travel-time-difference current meter. The measured steady-flow vertical-cosine-response used to calculate the predicted dynamic response is shown in the insert. (The low response at plus 70° is caused by the wake of the acoustic mirror.) (Measured data after Appell, 1977a.)

Figure 10

Measured dynamic response functions from four types of moored current sensors used in wave-zone studies. Measurements are plotted in the coordinates used previously. At the top, the response of an electromagnetic sphere (A) and an Aanderaa rotor-vane current meter (B) are shown for coplanar-circular-orbital motion (1.22 m diameter, three periods) superimposed on several linear tow carriage speeds. In the lower frame, performance of dual propellers (C) and acoustic-travel-time difference (D) flow sensors are shown for linear-sinusoidal motion normal to the tow.

In (A) note that for $\phi = 0°$, the measured dynamic response function is not constant as predicted by the kinematic model of Figure 5. This suggests that additional and dominant dynamic effects exist. [Data in (A) after Kalvaitis, 1977; (b) after Appell, 1977b; (c) after Davis and Weller, 1978; (d) is the same as shown in the previous figure.]

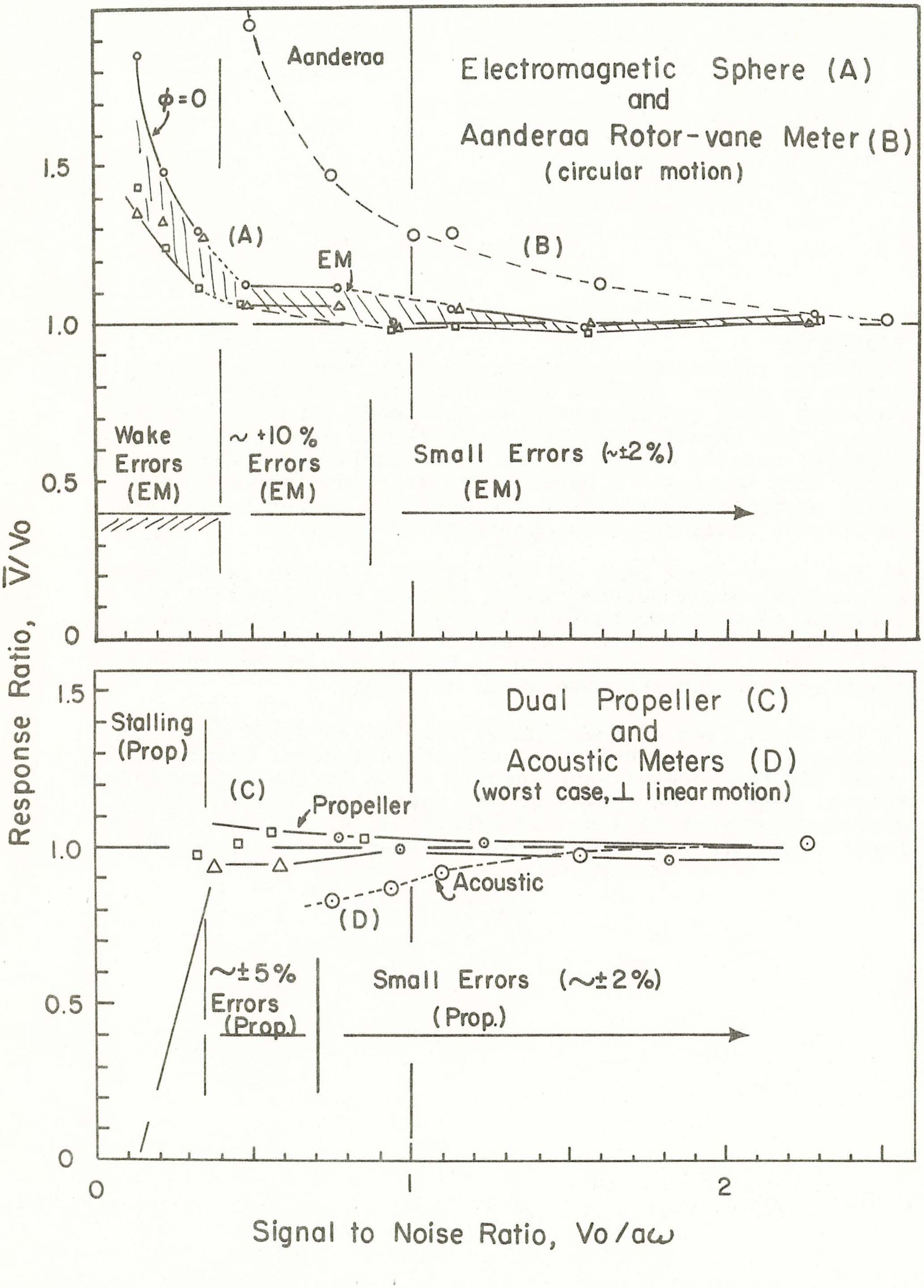
Electromagnetic Sphere (A)
and
Aanderaa Rotor-vane Meter (B)
(circular motion)
Aanderaa
φ=0
(A)
EM
(B)
Wake
Errors
(EM)
~ +10 %
Errors
(EM)
Small Errors (~±2%)
(EM)
1.5
1.0
0.5
0
Response Ratio, V̄/Vo
Dual Propeller (C)
and
Acoustic Meters (D)
(worst case, ⊥ linear motion)
Stalling
(Prop)
(C)
Propeller
Acoustic
(D)
~±5%
Errors
(Prop.)
Small Errors (~±2%)
(Prop.)
1.5
1.0
0.5
0
0
1
2
Signal to Noise Ratio, Vo/aω

Figure 11
Schematic representation of mean errors caused by mooring motion in waves. Perfect current meters (no error in measuring relative flow) are assumed. In the upper left part of the figure, the magnitude of Stokes-drift and errors caused by vertical mooring motion in the wave conditions indicated are shown as a function of depth. The stippled "current meter noise level" indicates that the mooring-induced errors are relatively small for this condition of swell.

At the upper right part of the figure, a simple zero-phase exponential-decay mooring model is used to illustrate the increase of both the horizontal and vertical oscillatory relative-motions (ΔU and ΔW) seen by moored instruments with depth. The wave "noise" seen by the meters increases with depth even though the wave sizes decrease.

In the lower part of the figure, the Stokes-drift and horizontal mooring-motion-induced current meter errors are shown for the modeled wave spectra shown in the insert (after Kenyon, 1969). The curves at the lower left are for fully developed seas of 20 knot (10 m/sec) winds, the pair at the lower right are for fully developed seas of 40 knot winds.

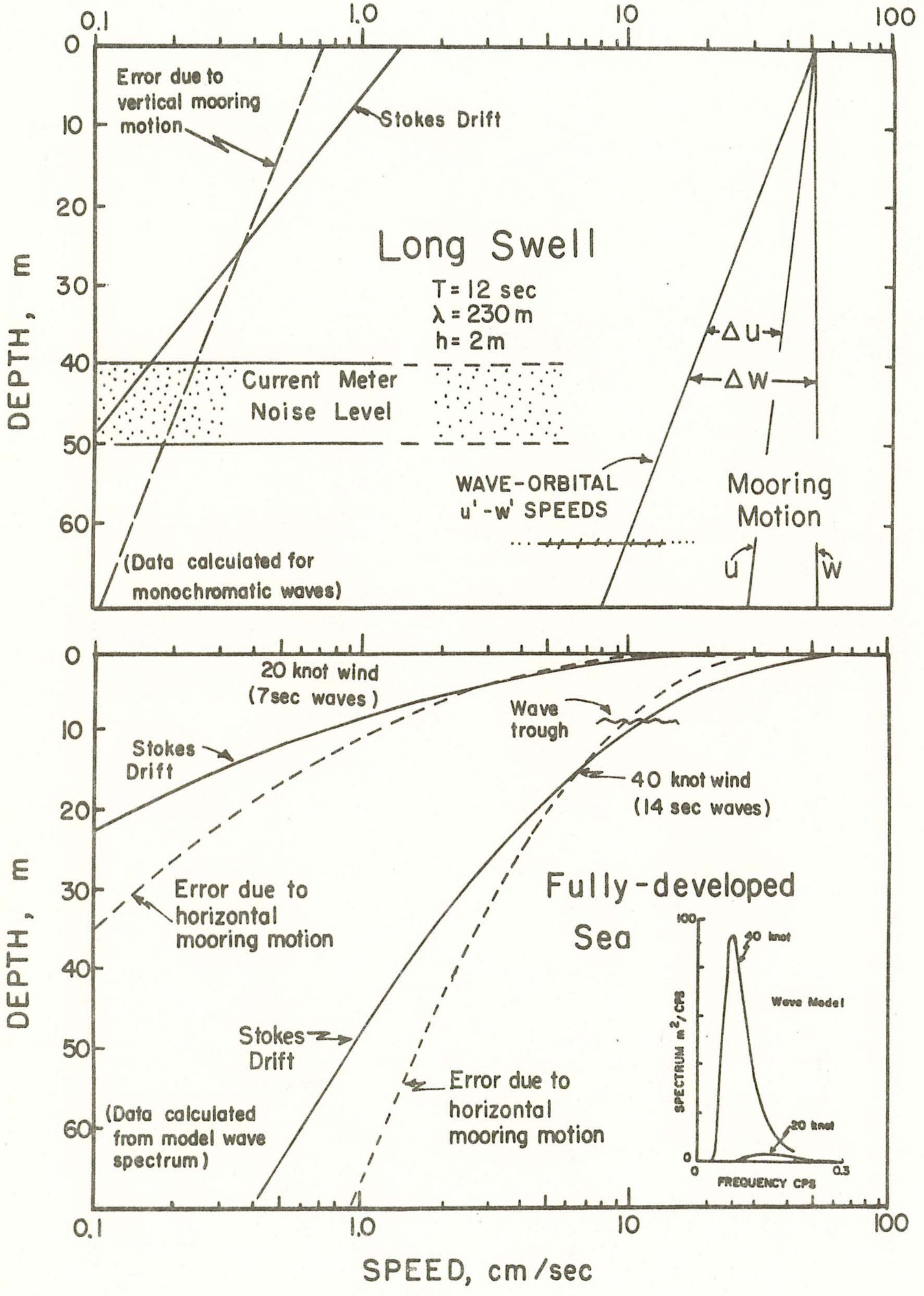
0.1
1.0
10
100
0
10
20
30
40
50
60
DEPTH, m
Error due to vertical mooring motion
Stokes Drift
Long Swell
T = 12 sec
λ = 230 m
h = 2 m
Δu
Δw
Current Meter Noise Level
WAVE-ORBITAL u'-w' SPEEDS
Mooring Motion
u
w
(Data calculated for monochromatic waves)
20 knot wind (7sec waves)
Stokes Drift
Wave trough
40 knot wind (14 sec waves)
Fully-developed Sea
Error due to horizontal mooring motion
Stokes Drift
Error due to horizontal mooring motion
(Data calculated from model wave spectrum)
100
SPECTRUM m²/CPS
40 knot
Wave Model
20 knot
0
0.3
FREQUENCY CPS
SPEED, cm/sec

undiminished with depth in the upper part of the mooring. The horizontal mooring motion component (u) is different, however, and can be modeled to first order as being equal to u' at the surface with an exponential decay (but at a slower rate than the waves) with depth. (The model of u shown is patterned after one developed by NDBO.) The oscillatory component of flow seen by current meters on the moving mooring is indicated by Δu and Δw in the figure. Note that the relative orbital motion typically increases, rather than decreases, with depth over the upper part of a surface-following mooring. Also, in the ocean mean currents typically decrease with depth. These wave, mooring, and ocean properties combine to produce favorable signal-to-noise ratios near the top and bottom of surface-following moorings, with generally poor signal-to-noise conditions at intermediate depths.

In the lower frame of Figure 11, errors due to horizontal-mooring-motion in 20- and 40-knot fully developed seas (see spectrum in insert) are predicted. The Stokes-drift conditions are included since they represent a second reasonable approximation to the errors caused by mooring motion.

The actual errors encountered will depend on both the mooring motion and its phase relative to the local wave flow. For this reason, error functions can not be predicted, even if the motion of the current meter is accurately known in space from other measurements such as pressure, acceleration, acoustic tracking, etc. The only hope then, for a first order mooring motion correction in waves, is through modeled mooring response and/or through direct measurement of the mooring motion and the relative values of u, v, and w at Nyquist frequencies high enough to resolve the wave motions. To reiterate:

- Current measurement errors due to mooring motion in waves exist even if ideal current sensors (ones with no errors) are used.
- Knowledge of the mooring motion alone does not allow first-order correction since the motion relative to the waves is required.

8. How Well Can We Do in Waves?

Figures 12 and 13 give some highlights of the CMICE-76 current meter intercomparison described by Beardsley *et al.* (1977). Figure 12 gives a side view of the line of six moorings set in February 1976 in 28 m of water, south of Long Island, New York.

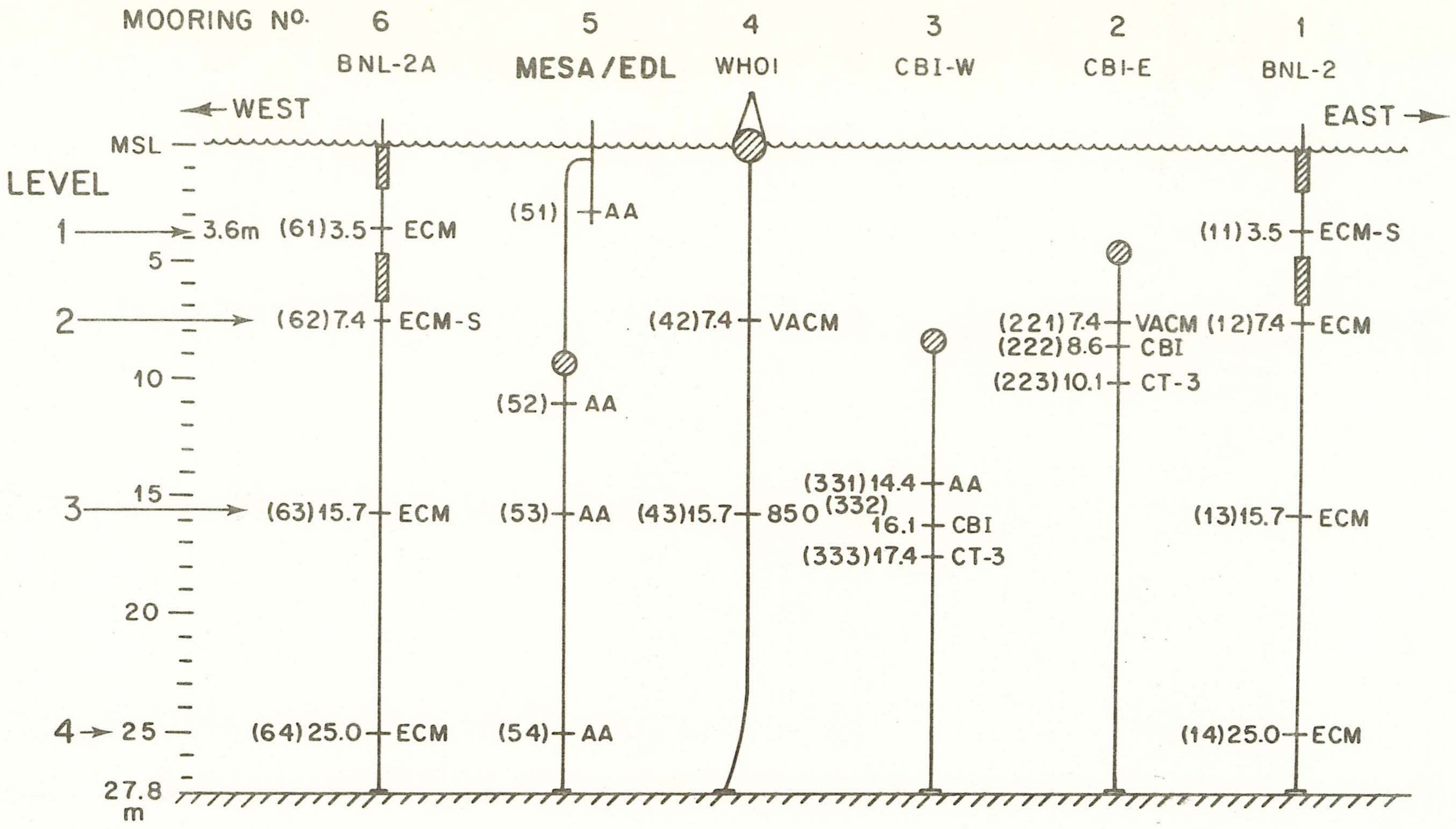

Figure 12

Mooring configuration of CMICE-76, a shallow-water near-surface current meter intercomparison. Moorings 1 and 6 are thin plastic spars tortionally fixed relative to the bottom and equipped with in-line electromagnetic sensors. Moorings 2, 3, and 5 are conventional subsurface types, while number 4 is surface-following. Mooring 5 has a small spar loosely tethered to the subsurface float. The moorings are in a line 1.1 km long placed parallel to shore, 5.9 km from shore, in 27.8 m of water. [Some of the abbreviations used are: CM = current meter, E = electromagnetic, S = spherical, AA = Aanderaa CM, CBI = modified Endeco CM, CT-3 = oriented electromagnetic CM, and (---) = instrument numbers. For further details see Beardsley *et al.*, 1977.]

Figure 13 gives comparative data from the 7.4 m depth level. Wave heights of 1 to 4 m were present during the experiment. The 15 scatter plots of one-hour vector-averaged current speeds (upper left) show (with the exception of the five CT-3 meter frames) a general agreement between the meters to within about ±10 cm/sec. Angular differences indicated by progressive vector diagrams (bottom right), however, may be large even when the speeds generally agree. Progressive vector diagrams of instrument numbers 12 and 62 (Figure 13) and the corresponding scatter plot (panel A) illustrate the problem. The differences in this case are thought to arise from the fixed-orientation mooring system and zero-stability properties of the electromagnetic current meters.

9. In Situ Testing

Moored intercomparisons of current meters at sea have been useful in identifying unanticipated differences between ocean current meter systems. Such tests, however, have not provided information on current meter accuracy, since the required in situ flow standards do not exist. Only relative performance is directly observed. Doppler current sensors on fixed platforms, acoustic ranges, etc., may one day provide the much needed standards for long-term in situ tests.

An interim test technique described by McCullough (1977) is shown in Figure 14. The plan view (top) and section view (bottom) show a 20 m-long, neutrally-buoyant boom, buoyed off horizontally at the desired test depth. One end of the boom is tethered to a moored boat, while the other end is free to swing with the current. Measurements of dye and drogue paths relative to the boom confirm that it aligns in waves to within a few degrees of the mean Lagrangian (Eulerian plus Stokes-drift) flow at its depth. The time of passage of dye past sensor stations at the middle and free-end of the boom is used to measure the advection speed of the dye patch. The possibility of tracing the advection of the horizontal temperature variability in a similar manner is being investigated.

Figure 15 shows sixteen pairs of dye observations starting at the upper left of the figure and ending at the lower right one hour later. For each trace pair, the mid-boom (station 1) signals have been aligned vertically. The delay to the end-boom (station 2) trace gives the Lagrangian speed estimate. A single hose with openings at stations one and two was used with a pump and recording fluorometer on board the

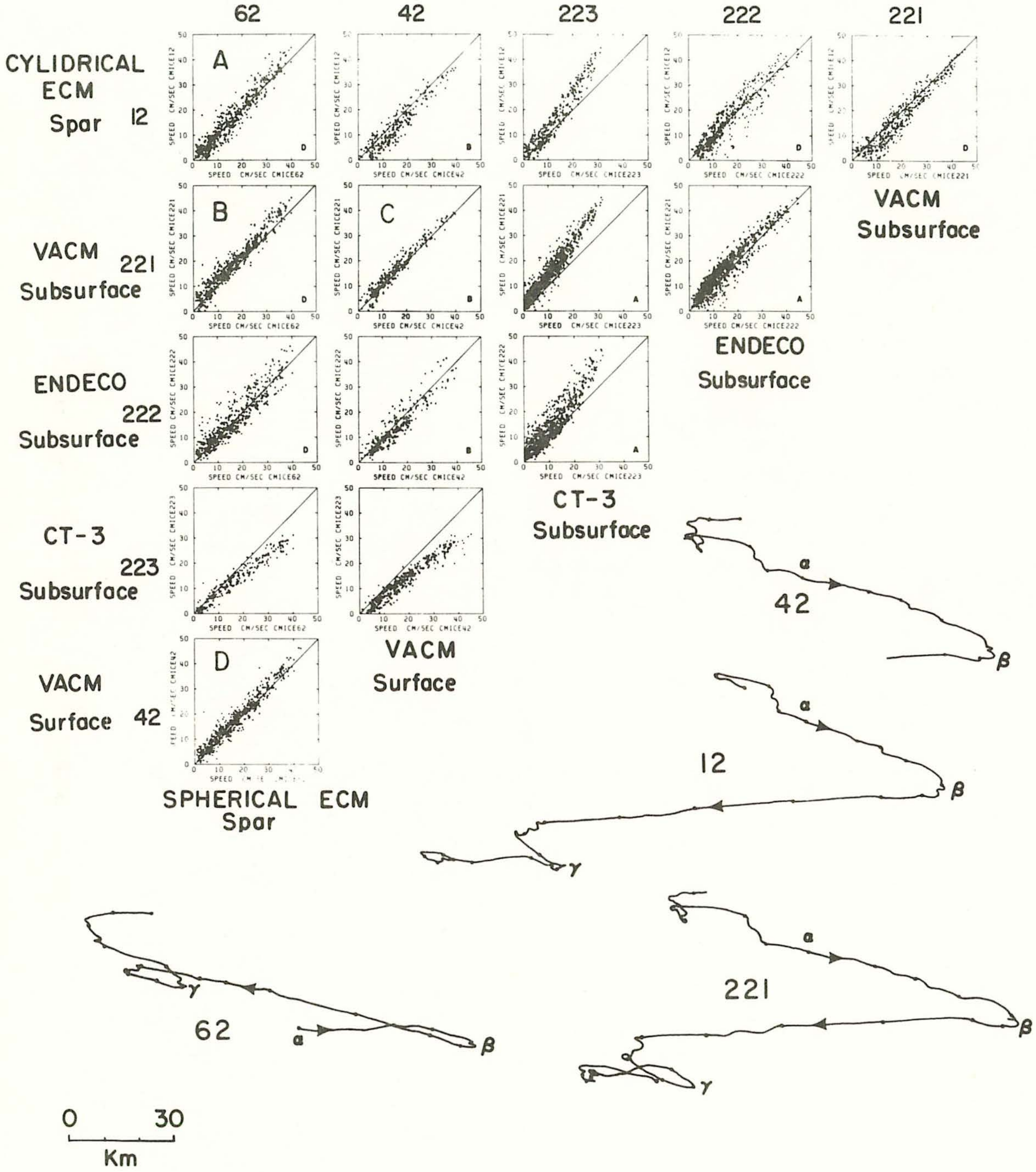
62
42
223
222
221
CYLIDRICAL ECM Spar 12
VACM 221 Subsurface
ENDECO 222 Subsurface
CT-3 223 Subsurface
VACM Surface 42
A
B
C
D
SPEED CM/SEC CMICE12
SPEED CM/SEC CMICE221
SPEED CM/SEC CMICE222
SPEED CM/SEC CMICE223
SPEED CM/SEC CMICE42
SPEED CM/SEC CMICE62
SPEED CM/SEC CMICE42
SPEED CM/SEC CMICE223
SPEED CM/SEC CMICE222
SPEED CM/SEC CMICE221
0
10
20
30
40
50
VACM Subsurface
ENDECO Subsurface
CT-3 Subsurface
VACM Surface
SPHERICAL ECM Spar
42
12
221
62
α
β
γ
0
30
Km

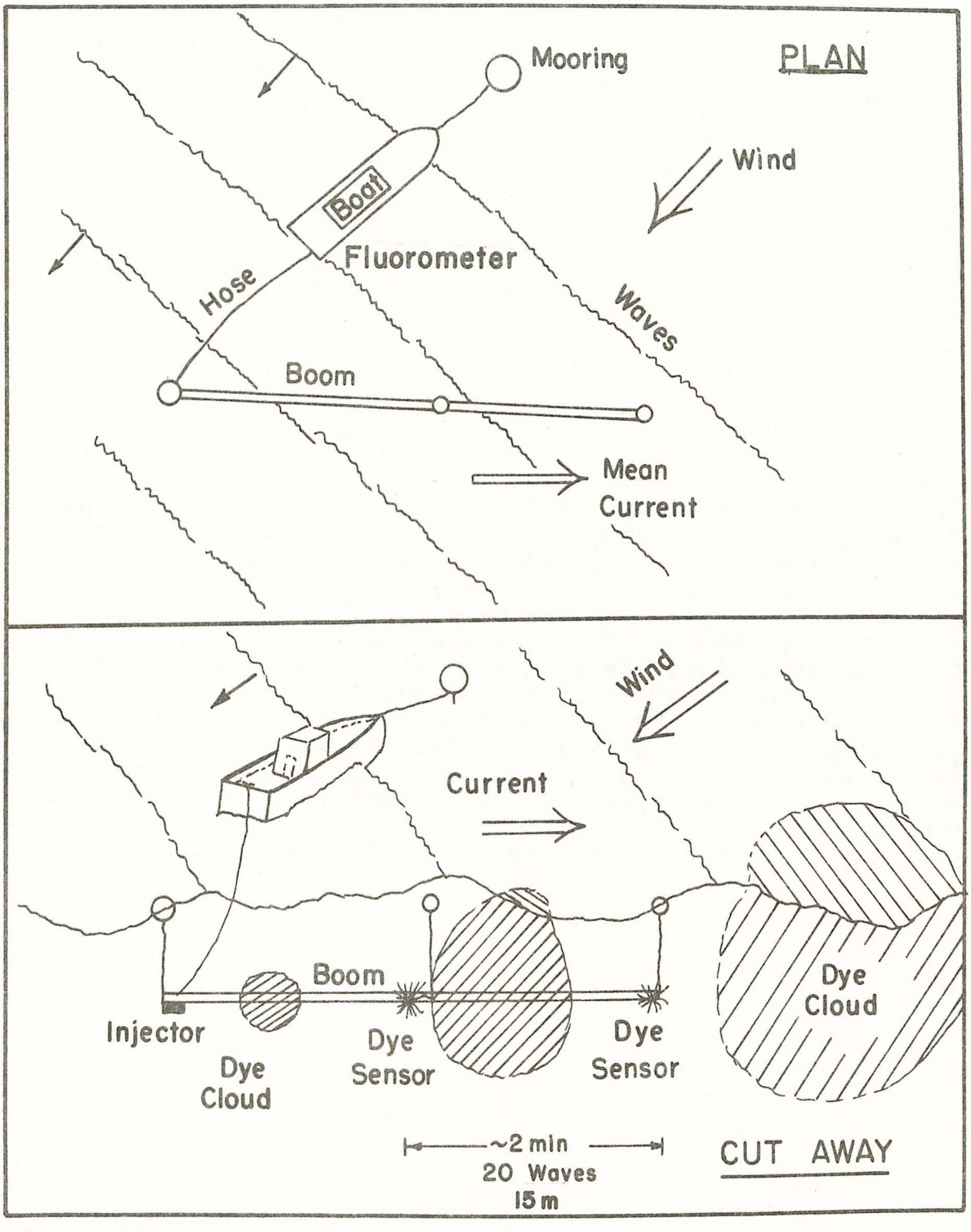

Figure 14

Sketch of an experimental dye technique used for in situ evaluation of moored current meters. A long submerged boom is loosely tethered at one end to a moored boat. Dye injected at the tethered end is advected away by the mean current. Its progress is measured at two dye sensor stations on the boom. The far end of the boom (at right) is free to swing with the current. Observations of wave conditions allow first-order Stokes-drift corrections needed to estimate Eulerian currents from the Lagrangian mean speed of the dye. (After McCullough, 1977.)

Figure 15

Dye concentration records from 16 dye injections over a period of one hour in small waves show the variation (wandering vertical line) in the mean tidal flow in Buzzards Bay, Massachusetts. Flow in the figure is from left to right. The actual flow direction during the experiment is estimated by measuring the bearing of the line of boom floats. Separation of the sensors along the boom was 15 m. The time between passage of the dye at the two stations is shown in minutes. The 16 trace pairs are separated by the elapsed time between dye injections of roughly 4 minutes. As shown by the scale below trace-pair 9, the mean dye speed was about 20 cm/sec. The scale also indicates how speed sensitivity increases at lower speeds. Variation of the dye intensity and multiple dye peaks are artifacts of the experimental procedure.

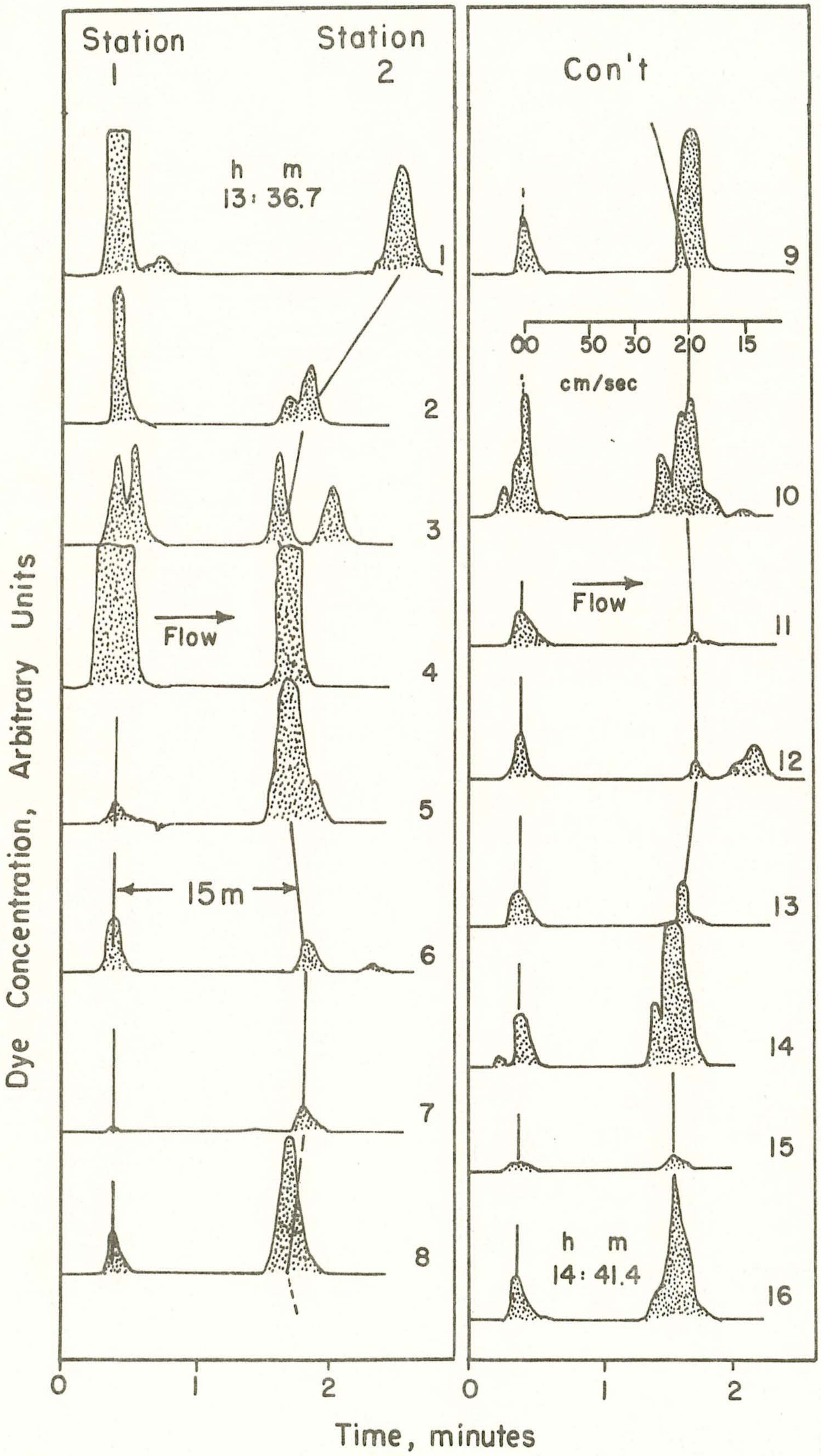
Station 1
Station 2
Con't
h m
13: 36.7
h m
14: 41.4
1
2
3
4
5
6
7
8
9
10
11
12
13
14
15
16
Flow
Flow
15m
00
50
30
20
15
cm/sec
Dye Concentration, Arbitrary Units
0
1
2
0
1
2
Time, minutes

boat to detect the dye passage. Absolute Lagrangian speed estimates accurate to perhaps ±1 cm/sec may be possible with the technique. Boom motion, asymmetric dye injection, limited number of dye sensors, and finite boom length are presently the major factors limiting accuracy.

Fundamental problems of relating the Lagrangian dye velocities to the Eulerian moored current meter observations exist, but as discussed earlier, they may not be critical in many practical situations. Since observations of currents from moving moorings are altered by effects similar to the Stokes-drift, intercomparisons of dye and moored current meter measurements may provide new insight into the accuracy of moored current meter observations from anchored but periodically moving platforms.

Acknowledgments

It is a pleasure to acknowledge the assistance of C. Herrity, W. Terry, A. Williams, and W. Woodward in the preparation of this paper. The work was supported by the Office of Naval Research under contract number N00014-76-0197 NR 083-004.

References

Appell, G. F., 1977a. Response characteristics of a prototype Neil Brown Instrument System, Inc. acoustic current meter (private communication).

Appell, G. F., 1977b. Current meter performance in a near-surface simulated environment. Exposure 5, 2.

Beardsley, R. C., W. Boicourt, L. C. Huff, and J. Scott, 1977. CMICE 76: A current meter intercomparison experiment conducted off Long Island in February-March 1976. Woods Hole Oceanographic Institution Technical Memorandum WHOI 77-62, 123 pp.

Carson, R. M. and P. G. Collar, 1977. On the measurement of near surface currents including the contribution from Stokes drift. I.O.S. Rept. No. 40, 37 pp (unpublished manuscript), 23 pp.

Davis, R. and R. Weller, 1978. Propeller current sensors. In NATO text, Instr. and Methods in Air-Sea Interactions, Ustaoset, Norway (preprint manuscript).

Halpern, D., 1977. Review of intercomparisons of moored current measurements. MTS-IEEE, Oceans-77, 2, 46D-1, 6.

Halpern, D., 1978. Moored current measurements in the upper ocean. In NATO text, Instr. and Methods in Air-Sea Interactions, Ustaoset, Norway (preprint manuscript).

Ianniello, J. P. and R. W. Garvine, 1975. Stokes transport by gravity waves for application to circulation models. J. Phys. Oceanogr., 5, 47-50.

Kalvaitis, A. N., 1977. Current sensor dynamic testing. POLYMODE News No. 28 (unpublished manuscript).

Kenyon, K. E., 1969. Stokes-drift for random gravity waves. J. Geophys. Res., 74, 6991-6994.

McCullough, J. R., 1974. In search of moored current sensors. MTS 10th Ann. Buoy Conf., Washington, DC, 31-54.

McCullough, J. R., 1975. Vector averaging current meter speed calibration and recording technique. Woods Hole Oceanographic Institution Technical Report WHOI 75-44, 35 pp.

McCullough, J. R., 1977. Problems in measuring currents near the ocean surface. MTS-IEEE, Oceans-77, 2, 46A,1-7.

McCullough, J. R., 1978. Techniques of measuring currents near the ocean surface. In NATO text, Instr. and Methods in Air-Sea Interactions, Ustaoset, Norway (preprint manuscript).

Neumann, G. and W. J. Pierson, Jr., 1966. Principles in Physical Oceanography. Prentice-Hall, 545 pp.

Pollard, R., 1973. Interpretation of near-surface current meter observations. Deep-Sea Res., 20, 261-268.

Shonting, D. H., 1967. Observation of particle motions in ocean waves. Naval Underwater Weapons Res. and Eng. Station, Newport, RI. Tech. Memo No. 377, vol. 1, 176 pp.

Smith, J. D., 1974. Turbulent structure of the surface boundary layer in an ice-covered ocean. Proc. of the 1972 ICES Symposium, edited by Talbot and Kullenberg, 53-65.

Webster, T. F., 1967. A scheme for sampling deep-sea currents from moored buoys. MTS 2nd Ann. Buoy Conf., Washington, DC, 419-431.

BIBLIOGRAPHIC DATA SHEET

1. Report No.
WHOI-79-90

2.

3. Recipient's Accession No.

4. Title and Subtitle
NEAR SURFACE OCEAN CURRENT SENSORS: PROBLEMS AND PERFORMANCE

5. Report Date
December 1979

6.

7. Author(s)
James R. McCullough

8. Performing Organization Rept. No.

9. Performing Organization Name and Address
Woods Hole Oceanographic Institution
Woods Hole, MA 02543

10. Project/Task/Work Unit No.

11. Contract/Grant No.

12. Sponsoring Organization Name and Address
NOAA Office of Ocean Engineering
Delaware Sea Grant College Program

13. Type of Report & Period Covered
Technical

14.

15. Supplementary Notes

16. Abstracts

When currents meters are used to measure mean horizontal currents in surface gravity waves, immunity to the vertical component of flow is important, even though the net vertical flow averages to zero and is normal to the desired horizontal components. A technique is presented for estimating the magnitude of the errors introduced by imperfect rejection of the off-axis flows (cross-talk) from laboratory measurements of the current meter "vertical-cosine-response." The predicted dynamic response is shown to compare favorably with laboratory measurements. The measured steady state vertical-cosine-response functions for several practical current sensors are summarized and used to estimate the magnitude of wave-induced errors in horizontal mean current measurements. A new dye technique for evaluating near-surface current meter performances in waves is shown.

17. Key Words and Document Analysis. 17a. Descriptors

1. Current meter
2. Dynamic response
3. Dye measurements

17b. Identifiers/Open-Ended Terms

17c. COSATI Field/Group

18. Availability Statement

19. Security Class (This Report)
UNCLASSIFIED

20. Security Class (This Page
UNCLASSIFIED

21. No. of Pages
27

22. Price

FORM NTIS-35 (REV. 3-72)

USCOMM-DC 14952-P72

Woods Hole Oceanographic Institution
WHOI-79-90

NEAR-SURFACE OCEAN CURRENT SENSORS: PROBLEMS AND PERFORMANCE by James R. McCullough. December 1979. 27 pages. Prepared for the Working Conference on CURRENT MEASUREMENTS sponsored by the NOAA Office of Ocean Engineering with the Delaware Sea Grant College Program.

When current meters are used to measure mean horizontal currents in surface gravity waves, immunity to the vertical component of flow is important, even though the net vertical flow averages to zero and is normal to the desired horizontal components. A technique is presented for estimating the magnitude of the errors introduced by imperfect rejection of the off-axis flows (cross-talk) from laboratory measurements of the current meter "vertical-cosine-response." The predicted dynamic response is shown to compare favorably with laboratory measurements. The measured steady state vertical-cosine-response functions for several practical current sensors are summarized and used to estimate the magnitude of wave-induced errors in horizontal mean current measurements. A new dye technique for evaluating near-surface current meter performance in waves is shown.

1. Current meter
2. Dynamic response
3. Dye measurements

I. McCullough, James R.
II. NOAA Office of Ocean Engineering
III. Delaware Sea Grant College Program

This card is UNCLASSIFIED

Woods Hole Oceanographic Institution
WHOI-79-90

NEAR-SURFACE OCEAN CURRENT SENSORS: PROBLEMS AND PERFORMANCE by James R. McCullough. December 1979. 27 pages. Prepared for the Working Conference on CURRENT MEASUREMENTS sponsored by the NOAA Office of Ocean Engineering with the Delaware Sea Grant College Program.

When current meters are used to measure mean horizontal currents in surface gravity waves, immunity to the vertical component of flow is important, even though the net vertical flow averages to zero and is normal to the desired horizontal components. A technique is presented for estimating the magnitude of the errors introduced by imperfect rejection of the off-axis flows (cross-talk) from laboratory measurements of the current meter "vertical-cosine-response." The predicted dynamic response is shown to compare favorably with laboratory measurements. The measured steady state vertical-cosine-response functions for several practical current sensors are summarized and used to estimate the magnitude of wave-induced errors in horizontal mean current measurements. A new dye technique for evaluating near-surface current meter performance in waves is shown.

1. Current meter
2. Dynamic response
3. Dye measurements

I. McCullough, James R.
II. NOAA Office of Ocean Engineering
III. Delaware Sea Grant College Program

This card is UNCLASSIFIED

Woods Hole Oceanographic Institution
WHOI-79-90

NEAR-SURFACE OCEAN CURRENT SENSORS: PROBLEMS AND PERFORMANCE by James R. McCullough. December 1979. 27 pages. Prepared for the Working Conference on CURRENT MEASUREMENTS sponsored by the NOAA Office of Ocean Engineering with the Delaware Sea Grant College Program.

When current meters are used to measure mean horizontal currents in surface gravity waves, immunity to the vertical component of flow is important, even though the net vertical flow averages to zero and is normal to the desired horizontal components. A technique is presented for estimating the magnitude of the errors introduced by imperfect rejection of the off-axis flows (cross-talk) from laboratory measurements of the current meter "vertical-cosine-response." The predicted dynamic response is shown to compare favorably with laboratory measurements. The measured steady state vertical-cosine-response functions for several practical current sensors are summarized and used to estimate the magnitude of wave-induced errors in horizontal mean current measurements. A new dye technique for evaluating near-surface current meter performance in waves is shown.

1. Current meter
2. Dynamic response
3. Dye measurements

I. McCullough, James R.
II. NOAA Office of Ocean Engineering
III. Delaware Sea Grant College Program

This card is UNCLASSIFIED

Woods Hole Oceanographic Institution
WHOI-79-90

NEAR-SURFACE OCEAN CURRENT SENSORS: PROBLEMS AND PERFORMANCE by James R. McCullough. December 1979. 27 pages. Prepared for the Working Conference on CURRENT MEASUREMENTS sponsored by the NOAA Office of Ocean Engineering with the Delaware Sea Grant College Program.

When current meters are used to measure mean horizontal currents in surface gravity waves, immunity to the vertical component of flow is important, even though the net vertical flow averages to zero and is normal to the desired horizontal components. A technique is presented for estimating the magnitude of the errors introduced by imperfect rejection of the off-axis flows (cross-talk) from laboratory measurements of the current meter "vertical-cosine-response." The predicted dynamic response is shown to compare favorably with laboratory measurements. The measured steady state vertical-cosine-response functions for several practical current sensors are summarized and used to estimate the magnitude of wave-induced errors in horizontal mean current measurements. A new dye technique for evaluating near-surface current meter performance in waves is shown.

1. Current meter
2. Dynamic response
3. Dye measurements

I. McCullough, James R.
II. NOAA Office of Ocean Engineering
III. Delaware Sea Grant College Program

This card is UNCLASSIFIED